Research Article | Vol. 9, No. 2 | 1 Feb 2019 | OPTICAL MATERIALS EXPRESS 400
Optical Materials EXPRESS

Non-stoichiometric grain-growth in ZnSe ceramics for $\chi^{(2)}$ interaction

X. CHEN[1,2,*] AND R. GAUME[1,2,3]

[1]*Department of Materials Science and Engineering, University of Central Florida, Orlando, Florida 32816, USA*
[2]*College of Optics and Photonics, University of Central Florida, Orlando, Florida 32816, USA*
[3]*NanoScience Technology Center, University of Central Florida, Orlando, Florida 32816, USA*
**xuan_chen_2013@knights.ucf.edu*

Abstract: Random quasi-phase-matching is a nonlinear scheme for three-wave mixing in transparent ceramics of non-centrosymmetric cubic materials. This process is controlled by the grain-size distribution of the ceramic and the nonlinear conversion efficiency is maximized when the average grain-size matches the coherence length. In this work, solid-state grain-coarsening is used to fabricate ZnSe ceramics with a desired grain-size. The effect of heat-treatment atmospheres (excess selenium vapor, zinc vapor or vacuum) on the grain-size distribution is investigated at 850°C and 1000°C and as a function of the heat-treatment time. The effect of these grain-size distributions on the efficiency of second-harmonic generation process by random quasi-phase-matching is analyzed theoretically.

1. Introduction

Three-wave mixing in nonlinear materials is a convenient way to generate new optical frequencies from common laser sources. Birefringent single-crystals are the most commonly used media for this process, but index dispersion limits their conversion efficiency unless the phase matching conditions are satisfied –by exploiting the birefringence phenomenon through angular orientation and proper temperature tuning. In the past two decades, the development of quasi-phase-matching (QPM) techniques involving periodically-poled, diffusion bonded [1,2] or epitaxially-grown materials, such as periodically-poled $LiNbO_3$ (PPLN) [3–5], orientation-patterned GaAs (OPGaAs) [6,7] or GaP (OPGaP) [8–10], have been extensively studied to alleviate this issue. The inversion of the sign of the nonlinear coefficient eliminates destructive interferences and allows the generated intensity to grow quadratically with the sample thickness. However, the techniques used to periodically flip the crystalline orientation remain fairly elaborate [11–13]. A third alternative consists of using transparent polycrystalline aggregates (ceramics) of non-centrosymmetric cubic materials. Despite the lack of long range order, these materials can serve as efficient nonlinear frequency converters by way of the random quasi-phase-matching (rQPM) process [14–16]. These process has been extensively studied both theoretically [17,18] and experimentally [19,20]. In these ceramics, the randomly-oriented crystallites all contribute to the nonlinear conversion process but with random phases and yet, the total contribution to the generated field is nonzero. Nonlinear conversion efficiency is maximized when the average grain-size of the ceramic is equal to the coherence length ($L_{coh} = \pi / \Delta k$) for the wavelengths of interest [21], i.e. when the distance over which the relative phase-lag of the three waves add up to π. The main feature of rQPM is the linear dependency of the frequency conversion yield with sample thickness. Although random quasi-phase-matching is less efficient than a phase-matched or quasi-phase-matched process, the difference is lessened in the femtosecond regime where short samples (<1 mm) are used. The current results on femtosecond second harmonic generation in ceramics can be found in recent reviews [20,22]. In addition, disordered polycrystalline media show a significant enhancement in spectral acceptance and

#340559 https://doi.org/10.1364/OME.9.000400
Journal © 2019 Received 2 Oct 2018; revised 4 Nov 2018; accepted 11 Dec 2018; published 3 Jan 2019

Optical Materials EXPRESS

tolerance to both propagation angle and temperature when compared to ordered crystals. With large second order susceptibility coefficients, small group velocity dispersion and wide transmission window from 0.45 to 21 μm, zinc selenide (ZnSe, cubic space group $F\bar{4}3m$) is ideal for accessing the MWIR and LWIR parts of the spectrum through rQPM nonlinear interaction [14–16]. The commercial availability of low-loss (bulk absorption coefficient at 10.6 μm is less than 0.0005 cm^{-1}) polycrystalline ZnSe infrared optics produced by chemical vapor deposition (CVD) [23,24] is yet another compelling factor for its use in rQPM devices [14,16].

This paper investigates heat-treatment conditions necessary to develop adequate microstructures for rQPM in CVD-grown ZnSe ceramics. Solid-state grain-coarsening of CVD-grown ceramics limits contamination from impurities compared to melt- or solution-grown crystals and hot-pressed ceramics. It also prevents the formation of scattering centers due to stress-induced birefringence and to the presence of hexagonal ZnSe when carried out below the sphalerite-wurtzite transition temperature at 1425°C. This study builds upon the previous work by K. Terashima *et al.* [25–27], R. Triboulet *et al.* [28–32] and Q. Ru *et al.* [15,16] in which heat-treatments were performed on CVD-grown ZnSe for the production of single-crystals and ceramics with controlled microstructure. Here, the effects of heat-treatment atmosphere [33] on the average grain-size and grain-size distribution are more specifically investigated and the experimentally-determined grain-size distributions are used to predict the rQPM efficiency of second-harmonic (SH) generation at an incident pumping wavelength of 4.7 μm and SH at 2.35 μm.

2. Experimental

Polycrystalline coupons of CVD-grown ZnSe (II-VI Inc., USA) with an average grain size of 75 μm were used as a starting material. Cubic samples measuring 5x5x5 mm^3 were diced from these coupons and all faces were mechanically polished so that grain-growth would not be suppressed [34]. Samples were annealed at 850 or 1000°C for 6 to 168 h in a vacuum, or in a saturated vapor pressure of zinc or selenium vapor. These vapors were produced by either placing fine zinc shots (Atomergic Chemetals Corp.) or selenium granules (United Mineral & Chemical Corp.) in a small boat next to the sample before sealing the quartz ampoule in which the treatment was performed. Ampoules were sealed off at a pressure of $3.4x10^{-6}$ atm. The microstructure of polished ZnSe was inspected by polarized optical microscopy after a 15 min chemical etch in a 30 mol% NaOH solution held at 95°C. The grain-size was determined by the line intercept method using the Image J software (National Institutes of Health). Grain-size distributions were obtained using a minimum of 1000 grains. Laser scattering tomography was used to check the precipitate after solid-state grain-coarsening [35–37]. Optical transmission was measured using an ultraviolet–visible–near infrared (UV–VIS–NIR) spectrometer (Cary 500, Varian Inc., CA, USA) and the mid-infrared transmission spectra were acquired on a FT-IR spectrophotometer (Nicolet 6700, Thermo Scientific).

3. Results and discussion

3.1 Grain-coarsening kinetics in CVD-grown ZnSe

Figure 1 shows the microstructures of ZnSe ceramics obtained before and after annealing under vacuum, Zn and Se vapors. As noticed previously [25,32], annealing in selenium vapor leads to the development of a coarser microstructure than in a zinc vapor or vacuum. Twining is present in all cases, even in the starting material. There is no significant difference in the amount of twins before and after grain-coarsening.

Optical Materials EXPRESS

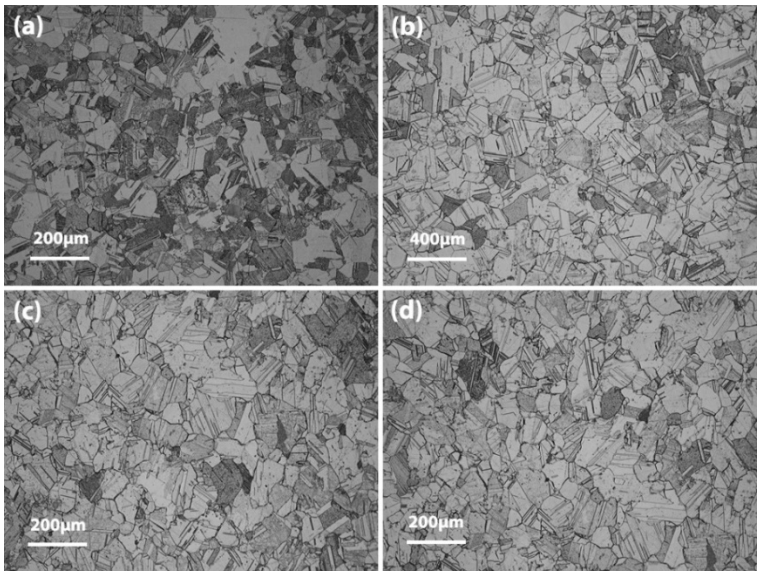

Fig. 1. Sample microstructures: (a) before annealing, (b) after annealing in Se vapor at 850°C for 168 h, (c) after annealing in Zn vapor at 850°C for 168 h, (d) after annealing in vacuum at 850°C for 168 h. Note the change of scale for figure (b).

The average grain-size as a function of annealing time is represented in Fig. 2 for different values of the temperature and atmosphere conditions. The error bars represent the 95% confidence interval for the population mean, calculated according to:

$$\bar{x} \pm t(\alpha, N-1) * \frac{s_x}{\sqrt{N}} \tag{1}$$

where $\bar{x}$ and s_x are the mean value and standard deviation of the sampled data set, respectively. With a grain population $N = 1000$, the significance level is α = (1-0.95)/2. The grain-growth kinetics is expected to follow a typical grain-growth model [38]:

$$d^m(t) - d^m(0) = k * t \tag{2}$$

where $d(t)$ is the average grain-size at time t, k a temperature-dependent factor and m the grain-growth exponent, with a value between 2 and 4. The fit to Eq. (2) yields $m = 3$ for a heat-treatment in Se vapor at 850°C, and $m = 6$ in the cases of Zn vapor and vacuum at the same temperature. In addition, it was found that the grain-growth exponent in Se atmosphere remains the same at 1000°C. In these conditions, crystallites as large as 1.5 mm can be obtained after 168 h of dwell time. Vapor transport equilibration affects the sample stoichiometry thereby modifies the diffusion rate of species and the mobility of grain-boundaries. The large grain-growth exponent found for the heat-treatment in vacuum and zinc vapor suggest the presence of low-solubility precipitates that pin the grain-boundaries. This fact is supported by the high density of scattering centers revealed by laser scattering tomography in those latter samples (Fig. 3). This in accordance with the Zn-Se phase diagram published by I. Avetissov *et al.* [39] showing that the solid-solubility limit of Zn is ten times lower (~10^{-5} mol of Zn per mole of ZnSe) than that of selenium in zincblende ZnSe at 850°C. It is also noteworthy that the heat-treatment in selenium vapor reduces the density of native scatters in CVD-grown samples, which suggests that the starting material may actually be zinc-rich. Based on the data from Fig. 2(b), one can calculate the activation energy for grain-growth in presence of selenium partial pressure using:

Optical Materials EXPRESS

$$k = k_0 \exp(-\frac{E_a}{RT}) \quad (3)$$

where k_0 is the pre-exponential constant of the diffusion coefficient, E_a the activation energy for grain-growth, T the absolute temperature and R the perfect gas constant. Using the grain-size data over the temperature range, an Arrhenius plot of Fig. 4 shows a mean activation energy value of $\overline{E_a}$ = 19.7 kJ/mol, similar to that reported by R. Triboulet *et al.* [32]. The coefficient of variation (CV) for the activation energy, defined as the standard deviation divided by the mean, is 7%, showing consistency within this data set. As the annealing time increases, the offset of the Arrhenius plot, ln(k_0), converges towards a single value suggesting that diffusion-driven grain-boundary mobility reaches an equilibrium across the entire sample size for long annealing times.

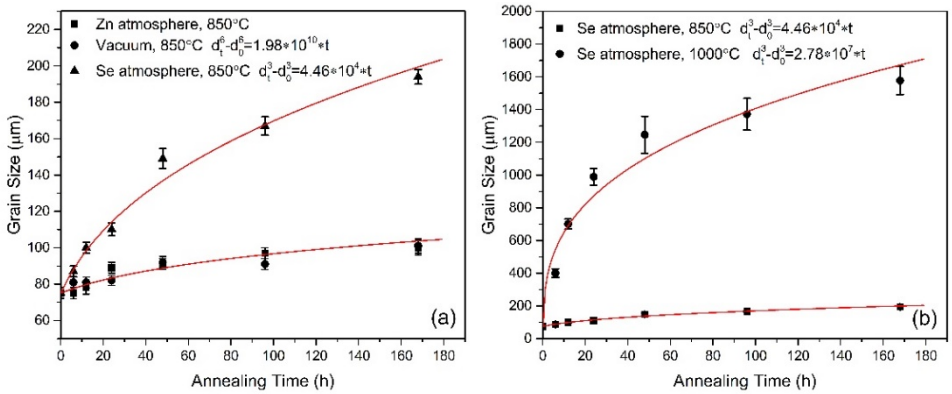

Fig. 2. Grain-size as a function of annealing time (a) at 850°C in different atmospheres, and (b) at 850°C and 1000°C in a Se vapor. d_0 = 75 µm.

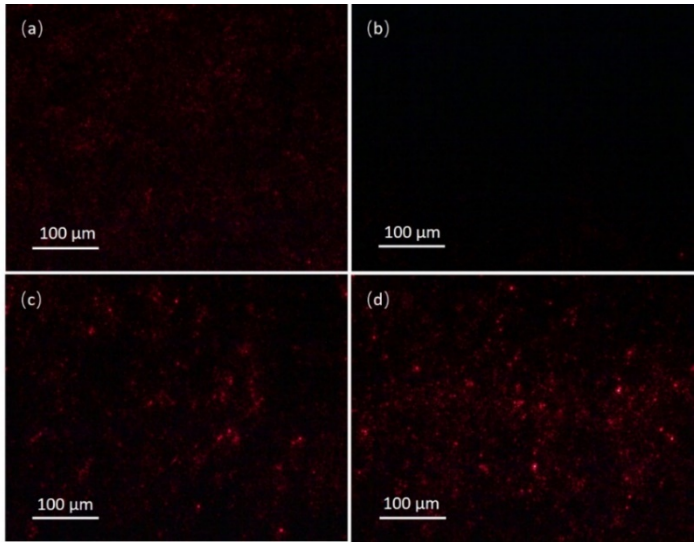

Fig. 3. Laser scattering tomography images of (a) original CVD-grown ZnSe ceramic and ZnSe ceramic samples annealed at 850°C for 168 h (b) in selenium; (c) in vacuum and (d) in zinc vapor.

Optical Materials EXPRESS

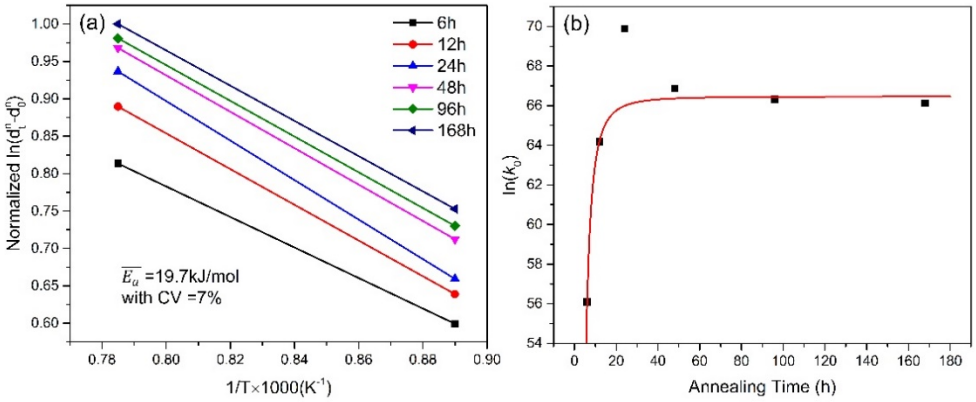

Fig. 4. (a) Arrhenius plot for ZnSe grain-growth kinetics and (b) ln(k_0) as a function of annealing time in Se vapor.

To analyze the effect of heat-treatment conditions on the grain-size distribution, we performed a comparison between heat-treated samples with the same average grain-size. This average grain-size was chosen to be 100 µm, *i.e.* a size optimized for MWIR random quasi-phase matched second harmonic generation at an incident pumping wavelength of 4.7 µm and SH at 2.35 µm. In a selenium atmosphere, 100 µm average grain-size is obtained after annealing at 850°C for 12 h. Conversely, a 168 h-long heat-treatment is necessary under vacuum or in a zinc atmosphere at the same temperature. Grain-size histograms (Fig. 5) were built using the Freedman-Diaconis rule to determine the binning size for data sets of N = 1000 grains, according to:

$$bin\ size = 2 * \frac{IRQ}{\sqrt[3]{N}} \tag{4}$$

where IRQ is the interquartile range of the data. These size histograms can be fitted to a lognormal distribution [40]:

$$f(d) = \frac{1}{\beta d\sqrt{2\pi}} \exp\left(-\frac{(\ln d - \alpha)^2}{2\beta^2}\right) \tag{5}$$

where d is the lognormally-distributed grain size, and α and β the mean and standard deviation of the logarithm of the grain size, respectively. The mean µ and standard deviation σ of the grain-size are respectively defined by:

$$\mu = \exp\left(\alpha + \frac{\beta^2}{2}\right) \tag{6}$$

$$\sigma^2 = \exp(2\alpha + \beta^2)[\exp(\beta^2) - 1] \tag{7}$$

Figure 5 shows that, regardless of the stoichiometry shift, the size-distribution remains lognormal with a similar standard deviation value. Therefore, the excess of selenium only favors a faster grain-growth compared to stoichiometric and zinc-rich ZnSe.

Optical Materials EXPRESS

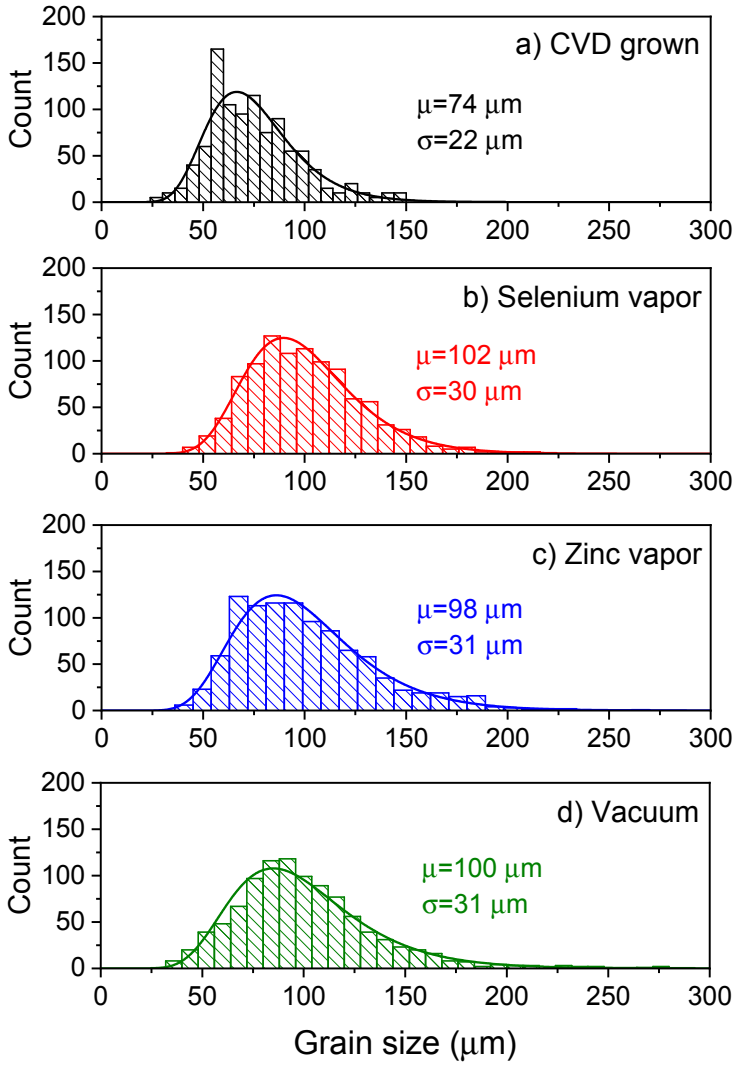

Fig. 5. Grain-size distributions of a) original CVD-grown ZnSe ceramics; and of annealed ceramics with comparable average grain-sizes (100 μm) after treatment at 850°C under b) Se vapor for 12 h, c) Zn vapor for 168 h and d) vacuum for 168 h. The mean grain-size value and its standard deviation are indicated for each fit.

It is worth noting that the off-stoichiometry defects introduced by heat-treatment in the presence of selenium deteriorate the transmittance of the samples in the near-infrared (Fig. 6). However, the color centers can be removed by a subsequent post-treatment at 700°C for 2 h in a vacuum. This short heat-treatment does not affect the average grain-size nor its distribution, and restores the transmittance to the level of the original CVD material (Fig. 6).

Optical Materials EXPRESS

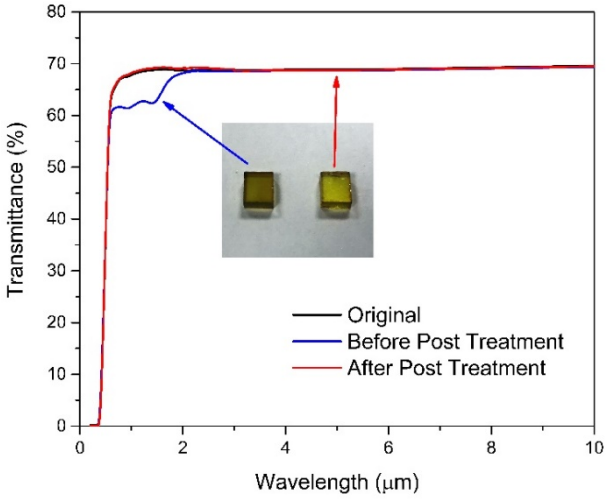

Fig. 6. Transmittance spectra of the starting CVD polycrystalline ZnSe, of a 12h-annealed sample in selenium vapor and of a 12h-annealed sample in selenium vapor consequently treated at 700°C for 2 h in a vacuum.

3.2 Effect of grain-size distribution on SHG efficiency

Random quasi-phase-matched second harmonic generation can be simply modeled using a one-dimensional (1D) layered structure along which light propagates and composed of grains with random crystalline orientations and thicknesses (Fig. 7). The refractive index and dispersion are assumed to be the same for all grains. One can show that, within the r^{th} grain, the electric field amplitude at frequency 2ω generated by the fundamental field is [21]:

$$E_{2\omega,r} = -\frac{\omega\chi_r^{(2)}}{n_{2\omega}c\Delta k}E_\omega^2\int_{Z_{r-1}}^{Z_r} e^{i\Delta kz}dz = -\frac{\omega\chi_r^{(2)}}{n_{2\omega}c\Delta k}E_\omega^2(e^{i\Delta kX_r}-1)e^{i\Delta k\sum_{j=1}^{r-1}X_j} \quad (8)$$

where c is the speed of light, $n_{2\omega}$ the refractive index at angular frequency 2ω, E_ω the electric field at the fundamental frequency, $\Delta k = k_{2\omega} - 2k_\omega$ the phase mismatch, X_r the size of the r^{th} grain and $\chi_r^{(2)}$ the effective nonlinear optical coefficient of grain r given its particular orientation.

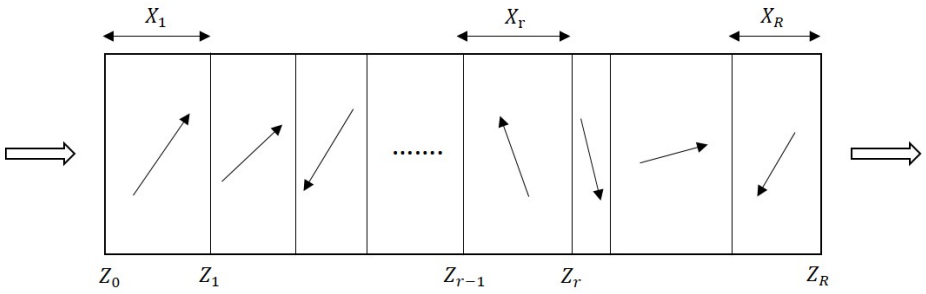

Fig. 7. Random quasi-phase-matching in a polycrystalline medium. Each block represents a crystallite with random thickness and crystallographic orientation. Light propagates through the thickness of this one-dimensional layered structure.

Optical Materials EXPRESS

The random orientation of the grains implies that the normalized component of the nonlinear polarization in the direction of the incident electric field ranges from 1 to −1. To implement this numerically, we used a random number generation algorithm so that $\chi_r^{(2)} = \cos(\pi y_r)\chi^{(2)}$ by sampling y_r uniformly in the interval [0, 1] [41]. After propagation through R crystallites, the amplitude of the electric field at 2ω can be deduced from Eq. (8):

$$E_{2\omega} = -\frac{\omega\chi^{(2)}}{n_{2\omega}c\Delta k}E^2(\omega)\left(\sum_{p=1}^{R}\cos(\pi y_p)\left(e^{i\Delta kX_p}-1\right)e^{i\Delta k\sum_{j=1}^{p-1}X_j}\right) \quad (9)$$

and the relative conversion efficiency is:

$$\frac{I_{2\omega}}{I_\omega} = \frac{n_{2\omega}\left|E_{2\omega}\right|^2}{n_\omega\left|E_\omega\right|^2} = \frac{\omega^2(\chi^{(2)}E_\omega)^2}{n_\omega n_{2\omega}c^2\Delta k^2}\left(\sum_{p=1}^{R}\cos(\pi y_p)\left(e^{i\Delta kX_p}-1\right)e^{i\Delta k\sum_{j=1}^{p-1}X_j}\right)^2 \quad (10)$$

For a given average grain-size, the effect of size-distribution on the conversion efficiency can be best determined using a Monte Carlo simulation [21]. Figure 8 shows the simulation results for a SHG process in polycrystalline ZnSe pumped at a wavelength λ = 4.7 μm at which the coherence length is 100 μm. In this figure, three cases are compared: (i) an ideal sample with a monodisperse grain-size of 100 μm, (ii) a sample having undergone grain-growth in selenium vapor with a size-distribution given by Fig. 5b (μ = 102 μm and σ = 30 μm) and (iii) the original CVD-grown ZnSe with 75 μm average grain-size (Fig. 5a). As expected, the conversion efficiency scales linearly with the number of grains, and the narrow grain-size distribution yields a higher conversion efficiency. The conversion efficiency of a selenium-treated sample reaches 83% of that of an ideal monodisperse microstructure and performs 62% better than an untreated CVD-grown ceramic.

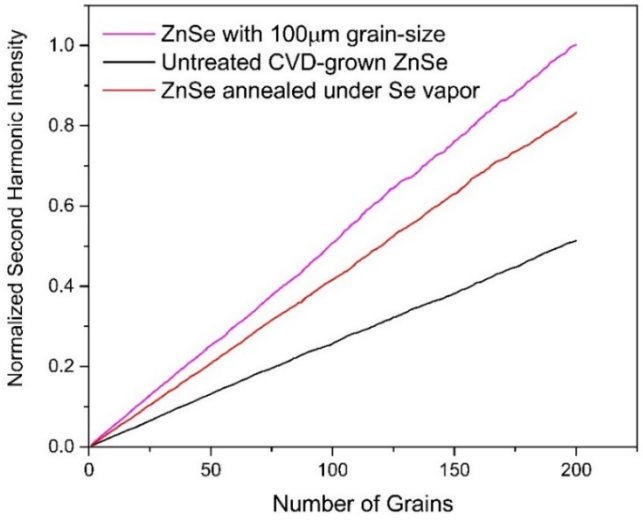

Fig. 8. Monte Carlo simulations of the normalized SH intensity as a function of number of grains for varied ZnSe ceramics (see text for details).

4. Conclusion

Solid-state grain-coarsening treatments of CVD polycrystalline ZnSe can be used to match the grain-size of this nonlinear material to the coherence length of a mid-IR pump. We have

Optical Materials EXPRESS

shown that the use of non-stoichiometric grain-growth heat-treatments allow for the control of the speed of the process and of the final grain-size distribution. When exposed to selenium vapor at 850°C, a faster homogeneous grain-growth could be obtained compared to treatments in a Zn vapor or a vacuum. We have quantified the effect of grain-size distribution in the process of random quasi-phase-matching and shown that the conversion efficiency scales linearly with the number of grains and a narrow grain-size distribution yields a higher conversion efficiency. Our Monte-Carlo simulations show that, for particular pumping conditions in the mid-infrared, the conversion efficiency of a selenium-treated sample could reach 83% of that of an ideal monodisperse microstructure and perform 62% better than an untreated CVD-grown ceramic.

Funding

Office of Naval Research (ONR) (N00014-15-1-2659).

References

1. L. Gordon, G. Woods, R. Eckardt, R. Route, R. Feigelson, M. Fejer, and R. Byer, "Diffusion-bonded stacked GaAs for quasiphase-matched second-harmonic generation of a carbon dioxide laser," Electron. Lett. **29**(22), 1942–1944 (1993).
2. D. Zheng, L. Gordon, Y. Wu, R. Route, M. Fejer, R. Byer, and R. Feigelson, "Diffusion bonding of GaAs wafers for nonlinear optics applications," J. Electrochem. Soc. **144**(4), 1439–1441 (1997).
3. L. E. Myers, R. Eckardt, M. Fejer, R. Byer, W. Bosenberg, and J. Pierce, "Quasi-phase-matched optical parametric oscillators in bulk periodically poled LiNbO 3," J. Opt. Soc. Am. B **12**(11), 2102–2116 (1995).
4. L. E. Myers, R. C. Eckardt, M. M. Fejer, R. L. Byer, and W. R. Bosenberg, "Multigrating quasi-phase-matched optical parametric oscillator in periodically poled LiNbO(3)," Opt. Lett. **21**(8), 591–593 (1996).
5. L. E. Myers, G. D. Miller, R. C. Eckardt, M. M. Fejer, R. L. Byer, and W. R. Bosenberg, "Quasi-phase-matched 1.064-microm-pumped optical parametric oscillator in bulk periodically poled LiNbO(3)," Opt. Lett. **20**(1), 52–54 (1995).
6. K. Vodopyanov, M. Fejer, X. Yu, J. Harris, Y.-S. Lee, W. C. Hurlbut, V. Kozlov, D. Bliss, and C. Lynch, "Terahertz-wave generation in quasi-phase-matched GaAs," Appl. Phys. Lett. **89**(14), 141119 (2006).
7. K. L. Vodopyanov, O. Levi, P. S. Kuo, T. J. Pinguet, J. S. Harris, M. M. Fejer, B. Gerard, L. Becouarn, and E. Lallier, "Optical parametric oscillation in quasi-phase-matched GaAs," Opt. Lett. **29**(16), 1912–1914 (2004).
8. P. G. Schunemann, L. A. Pomeranz, and D. J. Magarrell, "Optical parametric oscillation in quasi-phase-matched GaP," in *Nonlinear Frequency Generation and Conversion: Materials, Devices, and Applications XIV*, (International Society for Optics and Photonics, 2015), 93470J.
9. V. Tassev, M. Snure, R. Peterson, K. Schepler, R. Bedford, M. Mann, S. Vangala, W. Goodhue, A. Lin, and J. Harris, "Progress in orientation-patterned GaP for next-generation nonlinear optical devices," in *Nonlinear Frequency Generation and Conversion: Materials, Devices, and Applications XII*, (International Society for Optics and Photonics, 2013), 86040V.
10. V. Tassev, M. Snure, R. Peterson, R. Bedford, D. Bliss, G. Bryant, M. Mann, W. Goodhue, S. Vangala, K. Termkoa, A. Lin, J. S. Harris, M. M. Fejer, C. Yapp, and S. Tetlak, "Epitaxial growth of quasi-phase matched GaP for nonlinear applications: Systematic process improvements," J. Cryst. Growth **352**(1), 72–77 (2012).
11. C. Zhang, C. Wang, J. Yang, L. R. Dalton, G. Sun, H. Zhang, and W. H. Steier, "Electric poling and relaxation of thermoset polyurethane second-order nonlinear optical materials: Role of cross-linking and monomer rigidity," Macromolecules **34**(2), 235–243 (2001).
12. J. Xu, X. Lu, H. Chen, L. Liu, W. Wang, C. Zhu, and F. Gan, "Second harmonic generation investigation on electric poling effects in fused silica," Opt. Mater. **8**(4), 243–247 (1997).
13. L. L. Chang and K. Ploog, *Molecular beam epitaxy and heterostructures* (Springer Science & Business Media, 2012), Vol. **87**.
14. M. Baudrier-Raybaut, R. Haïdar, P. Kupecek, P. Lemasson, and E. Rosencher, "Random quasi-phase-matching in bulk polycrystalline isotropic nonlinear materials," Nature **432**(7015), 374–376 (2004).
15. Q. Ru, T. Kawamori, N. Lee, X. Chen, K. Zhong, M. Mirov, S. Vasilyev, S. B. Mirov, and K. L. Vodopyanov, "Optical parametric oscillation in a random poly-crystalline medium: ZnSe ceramic," in *Nonlinear Frequency Generation and Conversion: Materials and Devices XVII*, (International Society for Optics and Photonics, 2018), 1051615.
16. Q. Ru, N. Lee, X. Chen, K. Zhong, G. Tsoy, M. Mirov, S. Vasilyev, S. B. Mirov, and K. L. Vodopyanov, "Optical parametric oscillation in a random polycrystalline medium," Optica **4**(6), 617–618 (2017).
17. E. Y. Morozov, A. A. Kaminskii, A. S. Chirkin, and D. B. Yusupov, "Second optical harmonic generation in nonlinear crystals with a disordered domain structure," JETP Lett. **73**(12), 647–650 (2001).
18. E. Y. Morozov and A. S. Chirkin, "Stochastic quasi-phase matching in nonlinear-optical crystals with an irregular domain structure," Quantum Electron. **34**(3), 227–232 (2004).

Optical Materials EXPRESS

19. E. Sorokin and I. T. Sorokina, "Femtosecond operation and random quasi-phase-matched self-doubling of ceramic Cr: ZnSe laser," in *Lasers and Electro-Optics (CLEO) and Quantum Electronics and Laser Science Conference (QELS), 2010 Conference on*, (IEEE, 2010), 1–2.
20. S. Mirov, I. Moskalev, S. Vasilyev, V. Smolski, V. Fedorov, D. Martyshkin, J. Peppers, M. Mirov, A. Dergachev, and V. Gapontsev, "Frontiers of mid-IR lasers based on transition metal doped chalcogenides," IEEE J. Sel. Top. Quantum Electron. **24**(5), 1–29 (2018).
21. X. Vidal and J. Martorell, "Generation of light in media with a random distribution of nonlinear domains," Phys. Rev. Lett. **97**(1), 013902 (2006).
22. A. Dubietis, G. Tamošauskas, R. Šuminas, V. Jukna, and A. Couairon, "Ultrafast supercontinuum generation in bulk condensed media," Lith. J. Phys. **57**(3), 113–157 (2017).
23. W. Stutius, "Growth and doping of ZnSe and ZnSxSe1-x by organometallic chemical vapor deposition," J. Cryst. Growth **59**(1-2), 1–9 (1982).
24. A. Kamata, H. Mitsuhashi, and H. Fujita, "Origin of the low doping efficiency of nitrogen acceptors in ZnSe grown by metalorganic chemical vapor deposition," Appl. Phys. Lett. **63**(24), 3353–3354 (1993).
25. K. Terashima, M. Kawachi, and M. Takena, "Growth of ZnSe crystals by nonstoichiometric annealing," J. Cryst. Growth **102**(3), 387–392 (1990).
26. K. Terashima, M. Kawachi, and M. Takena, "Characteristics of ZnSe crystals annealed under host atom atmospheres," J. Cryst. Growth **104**(2), 467–474 (1990).
27. K. Terashima, E. Tokizaki, A. Uedono, and S. Tanigawa, "Study of point defects in bulk ZnSe grown by nonstoichiometric annealing," Jpn. J. Appl. Phys. **32**, 736–740 (1993).
28. R. Triboulet, J. Ndap, A. El Mokri, A. T. Carli, and A. Zozime, "Solid state recrystallization of II-VI semiconductors: application to cadmium telluride, cadmium selenide and zinc selenide," Le Journal de Physique IV **5**, 141–149 (1995).
29. R. Triboulet, J. Ndap, A. Tromson-Carli, P. Lemasson, C. Morhain, and G. Neu, "Growth by solid phase recrystallization and assessment of large ZnSe crystals of high purity and structural perfection," J. Cryst. Growth **159**(1-4), 156–160 (1996).
30. S. Fusil, A. Zozime, R. Penelle, F. Grillon, C. Le Paven, A. Rivière, and R. Triboulet, "Grain growth of ZnSe recrystallized in the solid phase," in *Solid State Phenomena*, (Trans Tech Publ, 1998), 311–316.
31. E. Rzepka, J. Roger, P. Lemasson, and R. Triboulet, "Optical transmission of ZnSe crystals grown by solid phase recrystallization," J. Cryst. Growth **197**(3), 480–484 (1999).
32. R. Triboulet, "Solid state recrystallization: a promising technique for the growth of semiconductor materials," Cryst. Res. Technol. **38**(35), 215–224 (2003).
33. R. L. Holman, "Novel uses of gravimetry in the processing of crystalline ceramics," in *Processing of Crystalline Ceramics* (Springer, 1978), pp. 343–358.
34. P. Lemasson, J. Ndap, S. Fusil, A. Riviere, B. Qu'hen, A. Lusson, G. Neu, E. Tournie, G. Geoffroy, A. Zozime, and R. Triboulet, "New results and trends in the solid phase recrystallization of ZnSe," Mater. Lett. **36**(1-4), 162–166 (1998).
35. K. Moriya and T. Ogawa, "Growth history of a synthetic quartz crystal," J. Cryst. Growth **58**(1), 115–121 (1982).
36. P. Gall-Borrut, T. Rakotomavo, M. Boncoeur, M. Valin, and F. Guastavino, "Observation of defect structure in ceramic oxides by laser scattering tomography," in *Window and Dome Technologies and Materials II*, (International Society for Optics and Photonics, 1990), 54–59.
37. J. Donecker and M. Naumann, "Laser scattering tomography for crystal characterization: Quantitative approaches," Crystal Research and Technology: Journal of Experimental and Industrial Crystallography **37**, 147–157 (2002).
38. J. Burke and D. Turnbull, "Recrystallization and grain growth," Prog. Met. Phys. **3**, 220–292 (1952).
39. I. Avetissov, K. Chang, N. Zhavoronkov, A. Davydov, E. Mozhevitina, A. Khomyakov, S. Kobeleva, and S. Neustroev, "Nonstoichiometry and luminescent properties of ZnSe crystals grown from melt and vapor," J. Cryst. Growth **401**, 686–690 (2014).
40. C. Pande, "On a stochastic theory of grain growth," Acta Metall. **35**(11), 2671–2678 (1987).
41. W. H. Press, *Numerical Recipes 3rd edition: The Art of Scientific Computing* (Cambridge university press, 2007).